

Central Lancashire Online Knowledge (CLoK)

Title	Tribological assessment of lubricants used in hydrogen assisted diesel engines
Type	Article
URL	https://clock.uclan.ac.uk/54974/
DOI	https://doi.org/10.1177/13506501251324037
Date	2025
Citation	Newadkar, Prathamesh, Al-Fetyani, Ahmad, Rahmani, Ramin, Rahnejat, Homer, Calderbank, Graham John, Smith, Edward H, Taylor, Robert Ian and Lyne, Amanda (2025) Tribological assessment of lubricants used in hydrogen assisted diesel engines. Proceedings of the Institution of Mechanical Engineers, Part J: Journal of Engineering Tribology. ISSN 1350-6501
Creators	Newadkar, Prathamesh, Al-Fetyani, Ahmad, Rahmani, Ramin, Rahnejat, Homer, Calderbank, Graham John, Smith, Edward H, Taylor, Robert Ian and Lyne, Amanda

It is advisable to refer to the publisher's version if you intend to cite from the work.
<https://doi.org/10.1177/13506501251324037>

For information about Research at UCLan please go to <http://www.uclan.ac.uk/research/>

All outputs in CLoK are protected by Intellectual Property Rights law, including Copyright law. Copyright, IPR and Moral Rights for the works on this site are retained by the individual authors and/or other copyright owners. Terms and conditions for use of this material are defined in the <http://clock.uclan.ac.uk/policies/>

Tribological assessment of lubricants used in hydrogen assisted diesel engines

Prathamesh Newadkar¹, Ahmad Al-Fetyani²,
Ramin Rahmani¹ , Homer Rahnejat^{1,2}, Graham Calderbank²,
Edward Smith², Robert Ian Taylor²  and Amanda Lyne³

Proc IMechE Part J:
J Engineering Tribology
1–15
© IMechE 2025



Article reuse guidelines:
sagepub.com/journals-permissions
DOI: 10.1177/13506501251324037
journals.sagepub.com/home/pij



Abstract

This study investigates the tribological performance of lubricants used in hydrogen-assisted diesel engines with specific focus on their rheology, additives and the formation of tribo-films. While there are concerns about reduced lubricant viscosity and increased wear due to hydrogen combustion, the impact of hydrogen on lubricant quality and tribology in Internal Combustion Engines (ICEs) is a less-explored topic. As an initial step, this study provides an in-depth analysis of lubricant performance in diesel engines, both with and without hydrogen assistance. The study includes chemical evaluations, and controlled tribometric performance analysis of lubricants from refuse trucks after an operation interval equivalent to 2000 km. The results show marginal changes in the lubricant rheology with the use of hydrogen, but there are differences in frictional behaviour under mixed and boundary lubrication regimes. In addition, X-ray Photoelectron Spectroscopy (XPS) analysis shows variations in anti-wear additive adsorption on surfaces, with a noticeable difference between fresh and used oil samples, aligning with the lubricant analysis data. Despite a noticeable difference in measured friction in mixed and boundary regimes of lubrication, the chemical analysis and XPS results show only marginal differences in the anti-wear additive content and the associated tribofilms. The study demonstrates that changes in the chemical and rheological states of the lubricant affect frictional performance and interaction of additives with surfaces in mixed and boundary regimes of lubrication. Understanding these changes is crucial for the future development of suitable formulations for use in dual-fuel hydrogen-assisted ICEs.

Keywords

Hydrogen fuel, IC engine, lubricant chemistry, lubricant rheology, friction, MTM, XPS

Date received: 5 July 2024; accepted: 12 February 2025

Introduction

It is widely anticipated that hydrogen-assisted combustion will play an increasing role in generation of power for marine, mining, agriculture, construction, haulage, and stationary auxiliary power plants. The major advantage in using pure hydrogen fuelled internal combustion engines (HICEs) or dual fuel hydrogen internal combustion engines (ICEs) is the reduction of greenhouse gas emissions such as CO₂ and major air pollutants such as NO_x at the tailpipe, providing that it is produced from renewable energy sources.¹ Therefore, hydrogen can play an important role in the quest for achieving net-zero emission targets. Dual-fuel hydrogen-assisted ICEs are increasingly viewed as suitable substitutes for purely fossil-fuelled ICEs particularly in heavy duty vehicles (HDV) applications. These could address some of the shortcomings of alternative sources of clean power, such as intermittency in supply, limited power range and remoteness of sources of power generation. Therefore, hydrogen presents promise as a fuel for the ICEs.

Hydrogen is considered as an attractive alternative fuel for combustion due to its higher flame propagation speeds, albeit at a lower ignition energy. Nevertheless, presently there are challenges regarding the use of hydrogen as a fuel, primarily stemming from a lack of requisite infrastructure for its production using renewable methods, efficient storage and transportation. There are also concerns regarding lack of sufficient relevant regulatory guidelines and standards.²

¹Wolfson School of Mechanical, Electrical and Manufacturing Engineering, Loughborough University, Leicestershire, UK

²School of Engineering, University of Central Lancashire PR1 2XQ, Preston, UK

³ULEMCo Ltd, Aintree Retail & Business Park, Liverpool, UK

Corresponding author:

Ramin Rahmani, Wolfson School of Mechanical, Electrical and Manufacturing Engineering, Loughborough University, Leicestershire LE11 3TU, UK.

Email: R.Rahmani@lboro.ac.uk

Some of the early research on the use of hydrogen in ICEs was reported by Furuhashi and Fukuma³ and an overview of progress and challenges, particularly on the combustion of hydrogen, has been provided by Verhelst and Wallner⁴ and more recently by Stepien.⁵ Qin et al.⁶ have conducted an experimental study on H₂-diesel dual fuel ICE performance subject to different H₂ ratios. They noticed that addition of hydrogen causes an increase in combustion pressure peak (7.7%), as well as cumulative heat release rate (3.5%) at H₂ to diesel fuel ratio of 20%. However, they did not provide any insight into the impact on the quality of lubricant or other tribological issues.

There are relatively a limited number of studies on the impact of hydrogen combustion on the quality of lubricant and its rheology, as well as the effect on the tribology of various ICE conjunctions such as the piston-cylinder system, valve train and engine bearings. A study by Pardo-García et al.⁶ examined the effect of introducing hydrogen in a dual-fuel diesel-hydrogen ICE. It was shown that the presence of hydrogen in the fuel mixture reduces CO, HC and smoke. However, a notable consequence was the reduction of lubricant viscosity by as much as 26%. There was a decline in the Total Base Number (TBN) and an upsurge in the Total Acid Number (TAN) of the lubricant, which are indicative of increased contamination and oxidation. These findings were in line with the previous research by Mathai et al.⁷ which reported similar trends in the TBN and TAN values in the case of engines fuelled with a mixture of hydrogen and Compressed Natural Gas (CNG). Furthermore, metallic components such as Fe, Cu, Al, and Cr exhibited substantial increases in concentration within the lubricant. This indicated increased wear of engine components.⁸ As a result, the lifespan of hydrogen-fuelled ICEs is generally considered to be lower than their conventional hydrocarbon-fuelled counterparts.⁹

Rahmani et al.¹⁰ developed a novel integrated analytical thermodynamic and tribological analysis of hydrogen-fuelled ICEs, including fuel injection type, gas blowby and lubrication models (a multi-physics approach) to study in-cylinder combustion and tribological performance of hydrogen-fuelled engines in an integrated manner. They also showed that the degraded (sheared) lubricants with lower viscosity produced lower Friction Mean Effective Pressure (FMEP). The lower lubricant viscosity resulted in a reduction in hydrodynamic load carrying capacity of the contacts, leading to reduced lubricant film thicknesses and a longer duration of direct boundary friction. Thus, owing to the decrease in lubricant viscosity, conjunctive film thicknesses reduce to maintain the load carrying capacity, resulting in increased instances of direct boundary interactions and wear. Under these circumstances, the role of lubricant additives in the formation of low shear strength tribo-films becomes crucial. Clearly, an increase in the production of water, arising from hydrogen combustion not only affects the viscosity of the lubricant, but can also potentially affect the formation of critical tribo-film components, comprised of friction modifiers and anti-wear additives.¹¹ McQueen et al.¹² noted that tribo-film formation

can significantly impact friction and wear performance. Their experiments demonstrated the prompt formation of tribo-films with supplemental anti-wear additives in tandem with zincdialkyldithiophosphate (ZDDP). Temperature also emerges as a catalyst for tribo-film formation and its stability.^{13,14}

Some preliminary studies of surfaces have shown the influence of hydrogen combustion upon the formation of tribo-films. Verhelst and Sierens¹⁵ showed that the properties of engine oil were significantly affected. The concentration of various additives in the lubricant such as ZDDP, which is used as an anti-wear agent, was significantly reduced along with almost complete disappearance of esters. This was attributed to the ability of hydrogen in breaking down the double carbon-carbon bonds in the hydrocarbon-based lubricants. Although this possibility is noted, there is no direct evidence that pure hydrogen would penetrate the lubricant. Therefore, it is essential to study the formation of tribo-films, as well as lubricant rheology in the presence of hydrogen-assisted combustion.

The proliferation of research on dual-fuel hydrogen-assisted ICEs has largely concentrated on engine thermodynamic performance, engine efficiency and durability, and critical outcomes regarding emissions. The study of tribological performance, particularly lubricant performance in rheological terms, as well as in the formation of tribo-films have been somewhat lacking. This requires a multi-scale investigation from in-field trials to micro-scale lubrication and onto nanoscale tribo-film formation.¹⁶ Clearly, development of lubricants suitable for the new emerging engine technologies is critical for their optimal performance. This paper provides a comparative study of lubricant performance for diesel-fuelled, and dual diesel-hydrogen fuelled ICEs through an in-field study of a number of refuse trucks, undergoing their normal daily duty cycle. Small samples of used lubricant were siphoned from the trucks' engines, rheologically tested and subjected to precision mini-traction machine (MTM) tribometry, as well as X-ray photoelectron spectroscopy (XPS) of the tested surfaces. This is a comprehensive study, not hitherto reported in the open literature.

Methodology

In-field testing

Domestic waste is collected at regular periods of time by local authority refuse trucks traversing fixed routes. The trucks in the current study are powered by 7.7 litre 6-cylinder diesel ICEs. Two such trucks were used in the current field study; one using dual diesel-hydrogen fuel. At instances of high-demanded power, up to 20% of the fuel injected into the cylinders was hydrogen. The trucks mileage before the study ranged 45,000 to 52,000. They used the same route in their rounds. These trucks were operated by Aberdeen Local Authority, Scotland, UK with fixed scheduled round-trip routes and usage frequency. They were all subject to very similar operating conditions. This was further ensured

by telemetric monitoring of ECU (Electronic Control Unit) data. Small amounts of used lubricant (150 ml) were drained off from all the engines' oil sumps after a 2000 km interval. An oil change interval of approximately 15,000–20,000 km is recommended. Therefore, all the in-field investigation is carried out within this period and with the same lubricant volume with no change or refill. The rheological state of the lubricant was first measured to ascertain the changes, such as viscosity, that affect bulk lubricant film performance. The lubricant samples were then subjected to precise laboratory-controlled tribometry using an MTM. This was carried out to establish the bulk lubricant behaviour and to promote creation of tribo-films, the constituents of which were ascertained through X-ray photoelectron spectroscopy (XPS).

Experimental set-up

Valve train systems are the highest loaded contacts in ICEs and are subjected to elastohydrodynamic regime of lubrication (EHL). The cam-roller follower contact is often subjected to a varying slide-roll ratio.¹⁷ Therefore, an MTM with independent rotations of the ball and disc samples can be used to achieve representative slide-roll contact kinematic ratios. A PCS Instruments MTM was utilised for the tribometric studies. The ball and disc specimens were driven independently, whilst the generated friction was automatically measured and recorded throughout the testing process. A lubricant reservoir, termed a "pot reducer" in the MTM parlance was used to conduct the tests if the volume of lubricant sample was reduced. Without the pot reducer, more than 35 ml volume of lubricant sample was required. With the use of the pot reducer, the required sample volume could be as low as 10 ml. This is an important feature that allows for utilising small samples of lubricants taken from real operating vehicles without having to replenish the lubricant with the consequence of affecting the ongoing in-field tests.

The specimens employed comprised standard MTM 3/4" ball and a disc specimen kit. To obtain the desired Stribeck curves, required steps in the tests were implemented within the MTM software. A contact load of 65N was chosen for all tests. The maximum Hertzian contact pressure, representative of primary EHL pressure peak, is obtained as^{18,19}

$$P_{max} = \left(\frac{6WE^{*2}}{\pi^3 R^2} \right)^{1/3} \quad (1)$$

where, R is the radius of the ball and W is the applied

normal load and the composite (effective) Young's modulus of elasticity is:

$$\frac{1}{E^*} = \frac{1 - \nu_b^2}{E_b} + \frac{1 - \nu_d^2}{E_d} \quad (2)$$

in which, E and ν denote Young's modulus of elasticity and Poisson's ratio and subscripts b and d refer to the ball and the disc, respectively. Table 1 outlines the material and geometrical properties of the ball, and the disc samples used in the current study.

Based on the data presented in Table 1, the average Hertzian contact pressure is determined from Equation (1) to be 0.8 GPa, which is within the typical range expected for vehicular valve train cam tappet or roller contacts.^{17,20,21}

The MTM lubricant pot temperature was maintained at 100°C for all the tests to provide a representative contact temperature.²² Tribometric tests were carried out with selected lubricant samples from the aforementioned ICEs, collected at different mileages. The tests were carried out at a slide-roll ratio (SRR) of 50%, whilst the lubricant's speed of entraining motion was set to vary from 2010 mm/s to 10 mm/s with decrements of 20 mm/s. These are typical kinematic contact conditions encountered in valve train contacts.²² This range provided an initial full fluid film lubrication conditions at the higher speeds of entraining motion, which also allowed for minimising early onset of wear. Then, the reduction in speed was expected to lead to mixed or partial, and subsequently boundary regimes of lubrication. In this manner a Stribeck curve for each lubricant sample can be made. Additionally, commencing the tribometric tests from a higher entrainment speed allows for minimal running-in conditions, affecting the surface topography at the early stages of all the tests. This approach ensures that any potential wear of contiguous surfaces can be kept to a minimum, at least for most of the complete Stribeck test conditions. Table 2 provides a summary of the operating conditions used.

The intention was to remain within piezo-viscous elastic (EHL) fluid film regime of lubrication, which is experienced in highly loaded contacts of ICEs, such as those of valve train system and timing gears. To ascertain that the chosen conditions complied with this requirement, dimensionless elastic and viscous parameters were evaluated as follows:^{19,23}

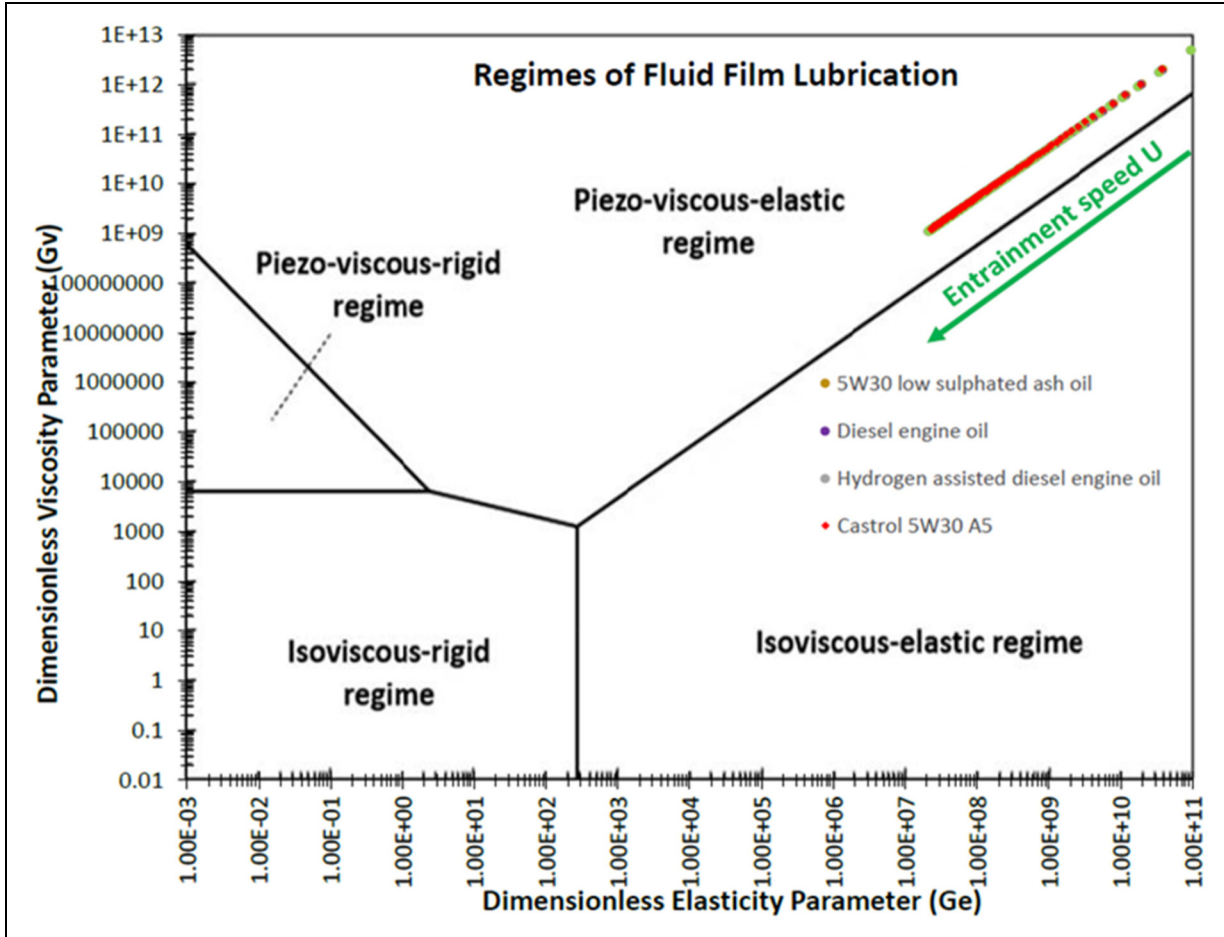
$$G_e = W^{*8/3} U^{*-2} \quad (3)$$

Table 1. Properties of the ball and disc samples used in the current study.

Property	Unit	Ball	Disc	Source
Material	–	AISI 52100	AISI 52100	Manufacturer specification
Diameter, D	mm	19.05	–	Manufacturer specification
Young's modulus of elasticity, E	GPa	207	207	Manufacturer specification
Poisson's ratio, ν	–	0.29	0.29	Manufacturer specification

Table 2. Operating conditions for the Stribeck tests.

Parameter	Symbol	Unit	Value/Range
Contact load	W	N	65
Entrainment speed	u	mm / s	0–2010
Slide-roll ratio	SRR	%	50
Temperature	T	°C	100

**Figure 1.** Fluid film regimes of lubrication.^{23,24}

$$G_v = G^* W^{*3} U^{*-2} \quad (4)$$

where, the dimensionless load, speed (rolling viscosity) and materials' parameters are given as:

$$W^* = \frac{W}{E'R^2} \quad (5)$$

$$U^* = \frac{u\eta_0}{E'R} \quad (6)$$

$$G^* = E'\alpha \quad (7)$$

in which, α is the lubricant's piezo-viscosity coefficient, u is the lubricant speed of entraining motion, and:

$$E' = 2E^* \quad (8)$$

Figure 1 shows the fluid film lubrication chart used to determine various regimes of fluid film lubrication, which was used in the current study for mapping the MTM operating conditions.^{23,24} The contact conditions listed in Table 1 were used to obtain and plot the dimensionless elastic and viscous parameters. The results plotted on the chart in Figure 1 show that the tribometric analysis remains entirely in the piezo-viscous elastic regime (elastohydrodynamic lubrication), as intended at the outset of all MTM tests. However, as the speed of entraining motion reduces, full film conditions are expected to alter to mixed and boundary regimes of lubrication.

Preparation of sample surfaces

The initial preparation of the existing specimen discs for the MTM tests involved the use of EcoMet 30 twin manual

grinding polisher, along with the application of silicon carbide polishing papers in the sequence: P320, P400, P600, and P1200 grits. Following the EcoMet 30 treatment, a thorough rinse was carried out to remove any residual debris from the surfaces of the discs. To polish the discs the Metaserv twin universal polisher was used multiple times. First the 6-micron pad was used and then to finish the 1-micron pad was used. The discs were once again cleaned to remove any loose material on the surface. The discs were then dried using acetone and blowing hot air in a desiccator for a period of approximately 10 min. The ball used was a standard MTM $\frac{3}{4}$ inch ball purchased from PCS Instruments with nominal Sa = 0.02 μm .

Topographical characterisation

After the completion of the disc polishing procedure, the topography and geometrical profiles of the discs were assessed using the Bruker NPFlex optical microscope, employing a white light interferometric (WLI) technique. A magnification factor of x20 was employed, with three measurements taken at the start of the tests. Subsequently, these measurements were imported into the Mountains Map v10 software tool, where the recorded surface curved profiles were removed, levelled, and a robust Gaussian filter was applied with a cut-off length of 0.25 mm. Average roughness of three measured location on each disc sample including the associated standard deviations are shown in Table 3. Figure 2 depicts examples of the measured surface topographical profiles prior to the tests carried out.

Tribofilm assessment by X-ray photoelectron spectroscopy (XPS)

Chemical analysis of MTM disc surfaces indicates the presence of various adsorbed/bonded elements, some of which are additives within the formulated lubricant and intended to facilitate certain functions in mixed and

boundary regimes of lubrication. Such additives may comprise anti-wear, friction modifier, antioxidant, detergents, and surfactants, to name but a few. With the increasing use, both the bulk rheological properties of the lubricant, such as its viscosity and the additive package can be subject to degradation or depletion. Therefore, the aim of surface analysis, post MTM tribometry using XPS, is to determine the extent to which various active elements are affected in different lubricant samples as indicated by their effectiveness in the formation of desired tribofilms. XPS is a highly effective and a pertinent technique for surface examination and wear scar characterisation due to its shallow probing depth of a few nanometres (~ 5 nm). The apparatus employed was the PHI Quantum 2000 system, featuring a robust monochromatic Al K α X-ray source with a photon energy of 1486.68 eV.

In the typical XPS analytical procedure, an initial survey scan was conducted to discern the chemical elements present within a probed region. Subsequently, high-resolution spectra of specific characteristic peaks, corresponding to each element were acquired to yield a more in-depth insight into the formed tribo-film's chemical composition, including the nature of chemical bonds formed. The acquired spectra were recorded in spatial mode. Deconvolution techniques were applied to discern distinct chemical species, and the C1s peak's position (284.8 eV) was employed for charge correction. Analysis was performed on the disc specimens both before and after the MTM tests. To ensure consistency in the acquired results, multiple measurements were undertaken both within and outside the wear track area. Specifically, three areas were analysed. For after test analyses, two areas on wear track and one area off-track were chosen for analyses. The XPS data obtained from high resolution scans were subjected to analysis using ThermoFisher's Scientific Advantage System for quantitative evaluation of the peak intensities and peak area sensitivity factors. This systematic methodology ensures

Table 3. Measured roughness parameters for the discs.

Disc / roughness parameter [nm]	Rq	Rz	Ra
Disc with fresh oil	3.19 ± 0.29	21.05 ± 1.62	2.49 ± 0.20
Disc with H ₂ engine oil	2.80 ± 0.35	17.50 ± 1.13	2.23 ± 0.29
Disc with diesel engine oil	3.29 ± 0.31	22.45 ± 1.11	2.58 ± 0.20

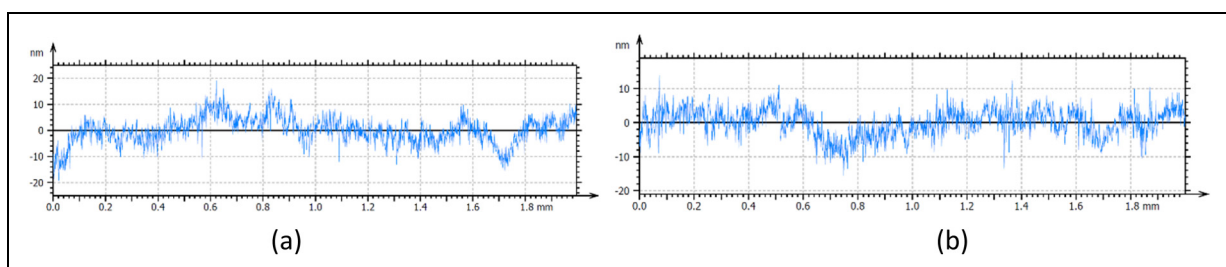


Figure 2. Examples of measured surface topography profiles after the polishing process.

accurate determination of the chemical constituents and properties of the formed tribo-films.

For the XPS system used, the maximum sample size was 60 mm×60 mm with a sample thickness of 20 mm. During the analysis, the X-ray beam was focused precisely onto the contact track. The contact patch radius can be determined using the Hertzian contact mechanics, with the contact footprint radius obtained as:^{18,19}

$$a = \left(\frac{3WR}{4E^*} \right)^{1/3} \quad (9)$$

Using the data in Table 1, the contact footprint radius is obtained as $a = 160 \mu\text{m}$. Therefore, areas encompassing $100 \mu\text{m} \times 100 \mu\text{m}$ in the contact wear track were used for XPS probing.

Characterisation of the lubricant samples

Samples of lubricant were siphoned from 2 refuse trucks powered by 7.7 l diesel engines and 2 refuse trucks with identical engines but modified to receive a mixture of diesel and hydrogen, with the latter accounting for a maximum 20% volumetric share at instances of peak or near-peak required power. The volumes of sampled lubricant from engines' sumps were kept to 150 ml after intervals of 2000 km. This sample size is sufficient for the subsequent investigations, including detailed chemical analysis of the lubricant and MTM tribometry. The volumes of siphoned lubricants were not replaced as this would have affected the integrity of the analyses.

All the lubricant samples taken from the engines along with a sample of fresh lubricant were chemically analysed for their rheological state, additive composition, contamination, and presence of wear metal content. Table 4 lists typical detailed chemical analysis content for the fresh lubricant, used lubricant samples from diesel powered trucks and those from dual-fuel diesel-hydrogen powered trucks. Such typical samples were used for the MTM tribometric investigations.

Table 4 shows that the viscosity at both 40°C and 100°C is higher for the used lubricants from both engine types when compared with the baseline fresh lubricant. This can be attributed to the accumulation of contaminants and oxidation products in the used/sheared lubricants. In addition, the oxidation and nitration, which are common indicators of degradation processes in engine oils, are higher in the used oils as would be expected.

The Total Base Number (TBN), which indicates the lubricant's ability to neutralise acids. This is typically higher in fresh lubricants due to the presence of alkaline additives, designed to neutralise acidic by-products and prevent engine corrosion. Over time, it is expected that TBN would be decreased as the additives are depleted. However, in the current results the TBN for the used oils and that of the fresh lubricant are barely different (within the measurement errors). This is again expected because the truck was in use for limited mileage.

The Total Acid Number (TAN), which is a measure of lubricant's acidity, is higher for the H₂-assisted engines similar to the findings in,⁶ indicating higher lubricant oxidation, thermal degradation, or contamination with acidic products. This is expected as combustion of hydrogen leads to increased production of acidic content. The diesel-operated engine lubricant shows little change in TAN in comparison to that of the fresh oil and is close the reported results elsewhere.²⁵

Boron is often used as an additive in engine oils due to its excellent anti-wear and antioxidant properties. However, the oil analysis results show significantly higher concentration of boron in the used engine oil samples. Considering that boron is also used in the additive package of engine coolants due to its corrosion-inhibiting properties, the higher concentration of boron in the used oils implies that there has been potentially some coolant leakage into the oil sump of the engines. However, glycol levels from the coolant, as shown in Table 4, are zero and therefore, possibility of cross-contamination from previous oil should be considered.

The existence of magnesium in the fresh oil sample is expected as it is a common detergent lubricant additive.

The concentrations of wear metals including aluminium, iron, chromium, and molybdenum are higher in the used oil samples, indicating propensity to potential engine wear. The higher levels in the H₂-assisted engine lubricant could suggest increased wear in this engine. Although the viscosity of the lubricant is only marginally altered with the presence of hydrogen (as shown in Table 4), under engine operating conditions the conjunctive surface temperatures are expected to be higher in the presence of hydrogen in the combustion process as it increases the heat release rate.⁵ This means that the operating viscosity of the lubricant could be lower than that shown in Table 4. As a result, with hydrogen combustion, transient viscosity of the lubricant would be lower, and thus the load carrying capacity would be reduced. This means more instances of direct interaction of surfaces can occur, leading to a rise in wear as indicated by the increased metallic debris with the hydrogen-assisted engine lubricants.

Calcium is often used as a detergent and dispersant to prevent engine deposits and sludge. It has acid neutralising properties, which is lower in the used oils compared with the fresh oil. This is expected because of the continuous consumption of calcium. It is also interesting to note that the drop in the calcium levels in the H₂-assisted engine oil (18.9%) is twice that for the diesel fuelled engine (9.72%). This points to some adverse effects of hydrogen on calcium consumption from the lubricant, which can be potentially attributed to the production of more acidic by-products (as is evident from the lower PH values) or higher operating temperatures in H₂-assisted diesel engine, which leads to faster oil oxidation, quicker accumulation of acids, and could account for the higher TAN and drop in calcium levels for the H₂-assisted engine. In addition, due to higher

Table 4. Typical results of chemical analysis of fresh and used sampled lubricants from the diesel and dual fuel hydrogen-assisted engines.

Parameter	Unit	Castrol 5W30 low sulphated ash fresh oil sample	Lubricant from diesel fuelled engine	Lubricant from H ₂ -assisted diesel fuelled engine
Fluid Condition				
Kinematic viscosity @40°C	mm ² /s	69.7	72.4	77.3
Kinematic viscosity @100°C	mm ² /s	11.9	12.2	12.7
Viscosity index	mm ² /s	168	167	164
Oxidation area	Abs/0.1mm	22.78	24.54	28.81
Nitration area	Abs/0.1mm	8.17	9.34	11.71
Sulphation	Abs/0.1mm	21.05	21.99	24.45
TBN	mg KOH/g	8.0	9.1	8.2
TAN	mg KOH/g	2.34	2.10	3.36
iPH	pH units	6.9	6.1	4.8
Miniflash	°C	197.5	203.0	206.0
Additives				
B (Boron)	mg/kg	2	15	27
Ba	mg/kg	0	0	0
Ca	mg/kg	2387	2155	1936
Mg	mg/kg	80	214	343
P	mg/kg	684	644	634
S	mg/kg	2670	2718	2497
Zn	mg/kg	814	773	784
Contamination				
Water	ppm	—	593	706
Na	mg/kg	0.9	2.9	2.4
K	mg/kg	13.0	13.0	10.0
Si	mg/kg	3.9	2.5	3.0
Li	mg/kg	0.3	0.5	0.4
Bio Diesel	%	<2	<0	<2
Diesel % in oil	%	<2	<2	<2
Glycol	%	0	0	0
Wear metals				
PQ index		10	10	10
Al	mg/kg	0.7	1.1	3.3
Sn	mg/kg	0.1	0.0	0.3
Pb	mg/kg	0.0	0.0	0.0
Cu	mg/kg	0.0	0.9	1.7
Fe	mg/kg	1.3	6.6	14.0
Cr	mg/kg	0.1	0.3	0.9
Mo	mg/kg	0.4	7.4	14
Ni	mg/kg	0.0	0.1	0.2
Mn	mg/kg	0.3	0.3	0.4

temperatures in the engine associated with hydrogen combustion can also increase TAN levels. All these can lead to a faster depletion of calcium.

Phosphorus, sulphur and zinc are key components of ZDDP (zinc dialkyldithiophosphate), which is a common anti-wear additive. All these elements are lower in the case of the used oil samples indicating a reduction of ZDDP. The only exception is the slightly higher sulphur content in the case of diesel-fuelled engines' lubricants. However, other factors can also affect the sulphur content which need to be considered. These include contribution of sulphur from the diesel fuel which can explain the higher sulphur content in the diesel-fuelled engines. The existence of H₂ in the case of the dual-fuel engines

might have contributed to the reduction of sulphur content and a corresponding increase in the TAN for hydrogen-assisted engines (Table 4).

Water contamination/dilution of lubricant is also detected in the used lubricant samples. Water dilution for the vehicles in highly humid areas such as in the UK is commonplace. The 19% higher content of the water in the H₂-assisted engine oil can be attributed to the production of water as a result of combustion of hydrogen.

Results and discussion

To ascertain the degree of repeatability of MTM tests, an "off-the-shelf" Castrol 5W30 A5 lubricant was used for

the Stribeck curve sweeps prior to the tests with the intended sheared/used lubricant samples. Figure 3 shows the results for the measured coefficient of friction against the speed of lubricant entrainment, after two repetitive sweeps. It is shown that repeating the MTM tests under the same load and temperature conditions provides a consistent set of results across the range of examined conditions. Some subtle differences are observed at relatively low speeds, where mixed regime of lubrication occurs. These differences can be attributed to marginal differences in the surface topographic features of discs and/or the variation of their topography during the experiment and any subsequent asperity interactions.

The selected lubricant samples, including the used lubricants from diesel-fuelled and hydrogen-assisted dual-fuelled engines were examined using MTM under the constant applied contact load of 65 N, temperature of 100 °C and slide-roll ratio of 50%. The lubricants used in both engines were Castrol 5W30 low sulphated ash fully formulated lubricants. The speed of entraining motion was varied (see Table 2). Similar to the repeatability tests, the sweep of entraining speed, commenced from higher values with gradual reductions. Figure 4 shows the results for all the tested lubricants. They indicate negligible differences at higher entraining speeds, where the lubricant viscosity is the most important parameter in bulk fluid film regime of lubrication. These cases pertain to piezo-viscous elastic condition (EHL) as were shown in Figure 1. Results in Table 4 show that the differences in the measured viscosity of lubricant samples are relatively small. Therefore, the measured coefficients of friction for all three lubricant samples are close in value at high speeds of entraining motion (Figure 4). However, as the speed is reduced, the differences in the coefficient of friction particularly between the used lubricants for pure diesel-fuelled engine and that for

H₂-assisted one become noteworthy. Friction with diesel engine lubricant remains higher than that of H₂-assisted lubricant when the entraining speed is reduced and the transition in the contact conditions from full fluid film lubrication to mixed and boundary regimes occurs. In addition, both used lubricants show lower friction in comparison to the fresh lubricant particularly as the operating conditions move toward mixed and boundary regimes of lubrication. One possible reason could be due to variations in the surface topographical changes during the tests. It is also possible that the formation of anti-wear tribofilm on the running track in the case of fresh oil which could help with elevating the coefficient of friction (ZDDP-based tribofilms tend to roughen the surface when the roughness is a nanometres scale^{26,27}). Similar argument can also be made in the case of H₂-assisted lubricant in which the lesser presence of adsorbed anti-wear additives on the surface in comparison to the case of diesel fuelled engine lubricant could potentially contribute to the lower boundary friction.

Table 5 shows the average wear track depth data for the disc samples investigated in this study. As it can be seen the differences in the wear depth of surfaces are relatively insignificant.

In addition, an example of the aerial image and cross-sectional view of the wear track after the MTM tests is shown in Figure 5. As it can be seen the wear of the surface is relatively minimal compared to the overall topography of the surface. It is also noteworthy that the track width matches quite well with the predicted track width of $2a = 320 \mu\text{m}$ from equation (9).

X-ray photoelectron spectroscopy (XPS) was used to analyse the chemical composition of MTM disc specimens' surfaces before and after the tribometric tests. All disc samples were analysed at 3 locations: 2 locations on the wear track and a point off the wear track. The

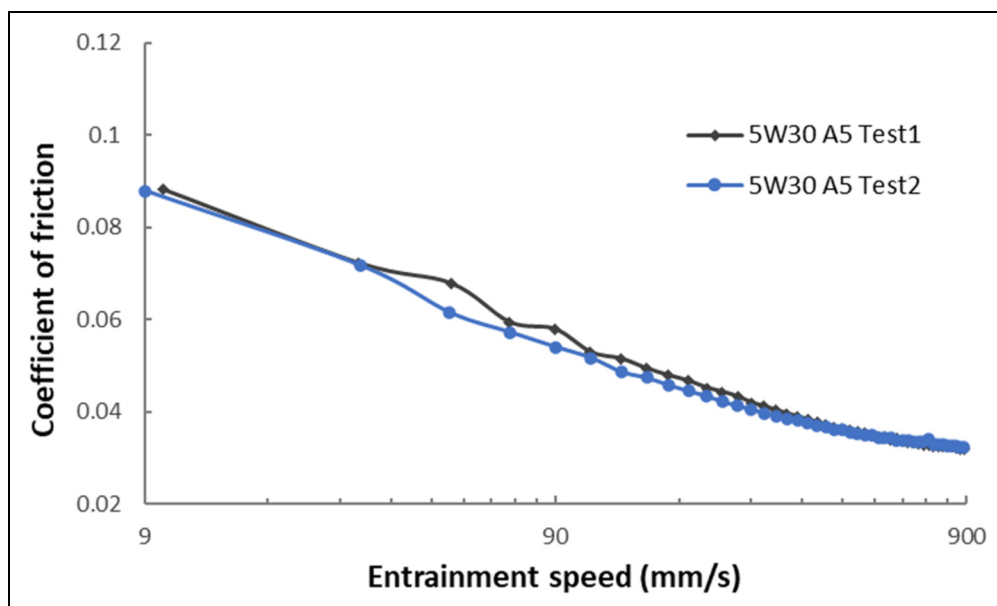


Figure 3. Stribeck curves to ascertain the degree of repeatability of the testing procedure (using samples of fresh lubricants).

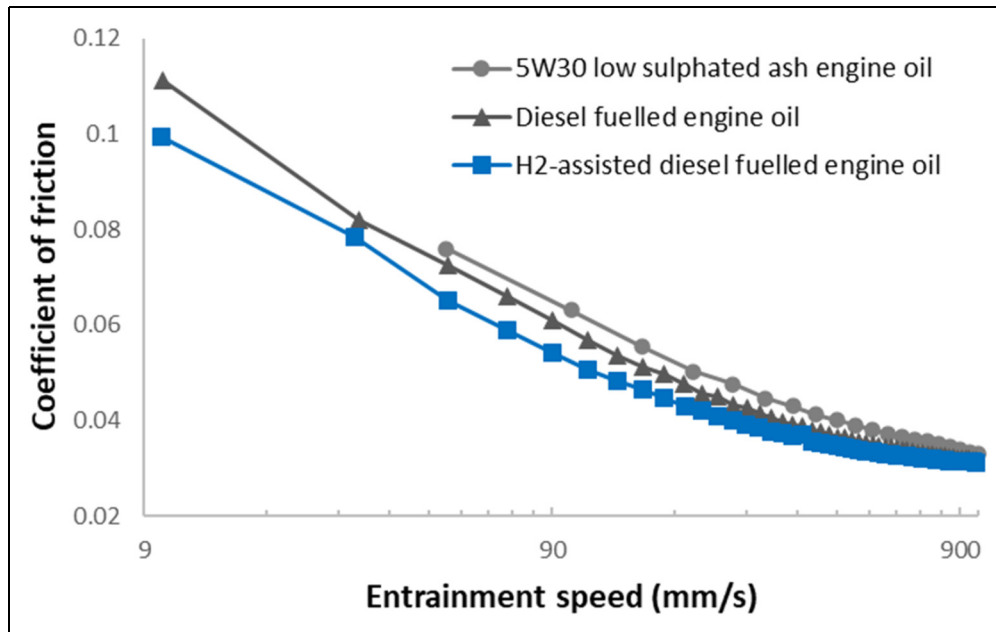


Figure 4. Stribeck curves for different lubricant samples in MTM tribometry with entrainment velocity variations in logarithmic scale.

surveys were conducted to find the composition of adsorbed/bonded elements, followed by a high-resolution spectral analysis to detect specific elemental details.

Tables 6 and 7 lists the results of elemental concentrations, including high resolution elemental analysis data, expressed as percentages obtained through XPS analysis of the MTM disc specimens, including those with the use of diesel engine oil and hydrogen-assisted dual-fuel engine oil. Table 6 reports on the results measured from off-track and Table 7 reports on the results measured from on-track locations on the discs, respectively. The tables also include the corresponding binding energies (BE) for all the detected elements. The results obtained from the wear track show the average of two measurements. In addition, Figure 6 shows the atomic percentages for the important additive species detected by the XPS on the tested surfaces.

The XPS analysis reveals specific chemical forms of various elements within the specimens. Calcium (Ca2p) was identified in its carbonate form, zinc (Zn2p) in its metallic state, sulphur (S2p) in the sulphate and sulphide forms, and phosphorus (P2p) in the phosphate bond configuration. The presence of sulphur in the form of sulphide, zinc, and phosphorous in the analyses provide strong evidence for the formation of a ZDDP (Zinc Dialkyl Dithiophosphate) tribo-film on the surface of the specimens.⁹

Oxygen (O1s) was detected in the analysis and found to exist in oxides, C=O organic, and C-O organic bonds, indicative of various chemical states and compounds formed during the decomposition and reaction of the ZDDP on the surfaces. The existence of high atomic percentage of oxygen (42.82%), indicates the presence of oxides, which is typical for polished steel surfaces. Carbon (C1s) was also identified and found to be

present in C-C, C-H, C-O-C, and C=O chemical bonds. Existence of carbon content with various carbon species suggests existence of oil residue on the surfaces. Furthermore, iron (Fe2p3) was detected in multiple forms, including Fe²⁺, Fe³⁺, and its metallic state.

The results from the virgin surface show that it primarily composed of oxygen, carbon and iron as would be expected of a steel surface subject to atmospheric conditions. The presence of calcium carbonate is mainly related to the exposure of the sample to fluid during the polishing process.

The results for surfaces after the tests with fresh 5W30 low sulphated-ash lubricant indicate that the lubricant additives have interacted with the surface during the tests, leading to changes in the surface composition. The presence of phosphate, zinc, and sulphide on the track-surface, post lubrication with the fresh lubricant can be attributed to the composition of the lubricant itself. Phosphorus and zinc are common additive constituents in engine lubricants and are used in zinc ester formulae like zinc dialkyldiphosphates (ZDDP). These form a protective film on the metallic surfaces in order to combat wear. Sulphur is also a common additive in the lubricants and is part of the SAPS (sulphated ash, phosphorus, and sulphur) content of the lubricant. Sulphur-based additives provide antioxidant and anti-wear properties. The presence of phosphate, zinc, and sulphide in the wear tracks indicates that these elements have interacted with the surface. The increase in the atomic percentages of these elements in the wear tracks, compared with those off-track, suggests that the interactions have been more intense in the areas of the surface that were subjected to high contact pressures and generated temperature, caused by shear under rolling and sliding conditions.

Comparison of off-track and on-track results also indicate that the operating temperature of 100°C may have not

been sufficient to cause traceable adsorption of phosphate, zinc, and sulphide on the examined sites of the surface, whilst the higher contact temperature and shear has provided sufficient activation energy to form these additive layers on the wear track.

The XPS examination of the surface after the tests with used 5W30 low-sulphated ash lubricant in the diesel-fuelled engine are also shown in Tables 6 and 7. The

Table 5. Measured wear track depth.

Oil sample used for test	Average depth of the wear track (nm)
5W30 low sulphated ash oil	5.0 ± 1.0
Diesel engine oil	5.0 ± 1.5
H ₂ assisted diesel oil	8.0 ± 1.0

presence of phosphate, zinc and sulphide in the wear tracks indicates that these elements from the lubricant have interacted with the surfaces similar to the case of the fresh oil and, and thus have formed a tribofilm. Again, the increase in the atomic percentages of these elements on the wear tracks compared with that off-track suggests that the interaction is more intense in the areas of the surface that were in contact with the ball during the tests, thus subjected to higher pressures and contact temperature.

A comparison of the results from fresh and used oils on the wear tracks show a noticeable reduction in phosphate, zinc and sulphide atomic percentages, indicating the depletion of surface-active additives, particularly ZDDP in the case of used oils.

There are some differences in the atomic percentages of oxygen (O1s) and carbon (C1s) between the XPS results on track for fresh and used oil samples. Higher

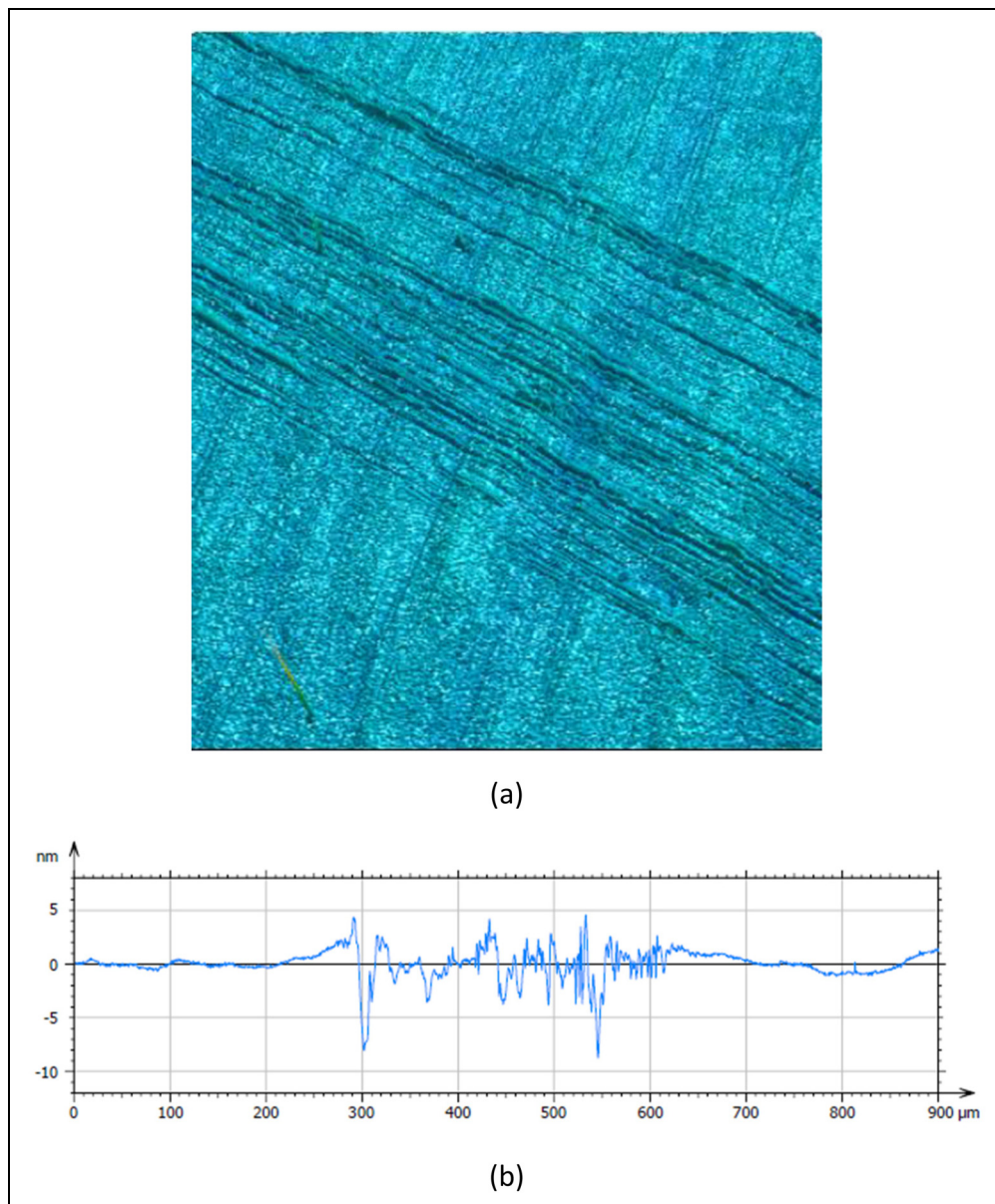


Figure 5. (a) An example aerial image and a cross-sectional surface profile view of the wear track after the experiment.

Table 6. XPS analysis of MTM specimen discs with elemental percentage concentration and the binding energies in eV (off wear track results).

Surface sample	Location	Atomic % and Peak Binding Energy [eV]	P2p Phosphate	Ca2p CaCO ₃	Zn2p Metal	S2p Sulphate	O1s Oxide	O1s Organic		C1s		Fe2p3	
								C=O	C-O	C-H	C-O-C		
Original (virgin) surface	on polished surface	Atomic %	—	1.61	—	—	42.82	—	—	13.85	—	33.99	
		Peak BE [eV]	—	348.26	—	—	531.27	—	—	285.05	—	—	708.54
Surface tested with Fresh oil (5W30 low sulphated ash)	off track	Atomic %	—	1.15	—	—	32.74	15.89	13.55	2.91	57.28	47.49	3.49
		Peak BE [eV]	—	346.85	—	—	531.14	529.44	531.14	532.80	284.76	284.76	286.27
Surface tested with used oil in diesel engine	off track	Atomic %	0.55	2.09	—	0.92	39.9	13.47	21.83	3.90	46.19	35.38	3.87
		Peak BE [eV]	133.56	347.41	—	168.72	531.43	529.60	531.43	532.80	284.84	284.84	286.45
Surface tested with used oil in H ₂ -assisted diesel engine	off track	Atomic %	—	1.54	0.99	0.57	36.21	17.44	18.98	4.53	51.56	32.92	3.31
		Peak BE [eV]	—	347.38	1021.72	169.18	531.35	529.65	531.43	532.80	284.76	284.79	286.43

Table 7. XPS analysis of MTM specimen discs with elemental percentage concentration and the binding energies in eV (wear track results).

Surface sample	Location	Atomic % and Peak Binding Energy [eV]	P2p Phosphate	Ca2p CaCO ₃	Zn2p Metal	S2p Sulphide / Sulphate	O1s Oxide	O1s Organic		C1s	C-O-C	C1s C-C, C-H	C1s C=O	Fe2p3
								C=O	C-O					
Original (virgin) surface	on polished surface	Atomic %	—	1.61	—	—	42.82	—	—	13.85	—	—	—	33.99
		Peak BE [eV]	—	348.26	—	—	531.27	—	—	285.05	—	—	—	708.54
Surface tested with Fresh oil (5W30 low sulphated ash)	wear track	Atomic %	—	1.84	2.66	1.97	—	4.76	43.60	2.80	32.99	3.46	3.45	7.54
		Peak BE [eV]	133.07	347.09	1021.76	161.66	—	529.48	531.03	532.80	—	284.79	286.32	288.36
Surface tested with used oil in diesel engine	wear track	Atomic %	1.26	1.28	1.01	0.48	—	11.49	19.07	2.61	—	45.87	2.91	6.16
		Peak BE [eV]	133.05	347.18	1021.72	168.95	—	529.63	531.28	532.80	—	284.58	286.38	288.42
Surface tested with used oil in H ₂ -assisted diesel engine	wear track	Atomic %	1.32	1.23	0.88	0.35	—	13.04	18.85	2.79	—	43.61	2.77	5.66
		Peak BE [eV]	133.13	347.29	1021.72	169.17	—	529.69	581.33	532.80	—	284.78	286.36	288.42

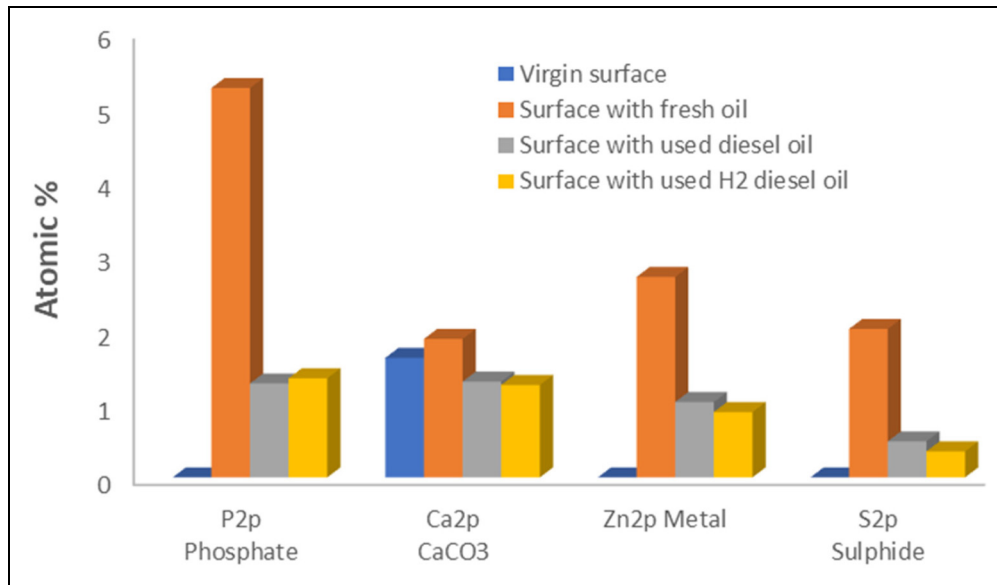


Figure 6. The atomic percentage of additive species on the tested surfaces with different lubricants.

overall atomic percentage of carbon (C1s) and a lower atomic percentage of oxygen (O1s) for the used oil samples compared with those for the fresh oil sample could be due to the degradation of the oil and accumulation of carbonaceous deposits (like soot) during use. In particular, the presence of C1s C-C, C-H with peaks around 284.8 eV with higher percentages of 45.875 and 43.61% for diesel fuelled and H₂ assisted engine oils compared with the 32.99% for the fresh oil can potentially imply the presence of hydrocarbons such as soot in the cases of used oils, in addition to the effect of normal oil residues on the samples. The existence of C1s C=O with 286.4 eV and atomic percentages of 6.16% and 5.66% for diesel fuelled and H₂ assisted engine oils compared to the 3.45% for the fresh oil indicates higher presence of carbonyl groups potentially as a result of oxidation and degradation in the used oil samples.

The atomic percentages of calcium carbonate (CaCO₃) and iron (Fe2p₃) (Tables 6 and 7) show relatively small differences between those from fresh and used oil samples, which can mainly be attributed to the differences in the polishing processes and the variations in the test conditions, as well as the number of spectroscopic tests.

A comparison of the additive elements between the off-track and wear track deposits indicates that the higher contact temperatures are not sufficient for the activation of zinc on the surface as was also observed in the case of the fresh oil. However, appreciable atomic percentages of phosphate and sulphide have been measured unlike the case for the fresh oil sample. Lubricant degradation over time and usage under harsh engine conditions occur due to thermal and oxidative stresses.²⁸ This degradation can lead to the formation of various compounds, including metal phosphates and sulphides, which can then be adsorbed onto the steel surfaces leading to the detection of these elements through XPS analysis.

The higher BE for S2p in surfaces tested with used oil indicates the formation of sulphates rather than sulphides.

The formation of sulphates suggests oxidative conditions within the lubricant during use in engines. Sulphates are expected to typically form due to oxidation of additives which contain sulphur. This oxidation process can be an indicative of the lubricant's degradation over time. These findings indicate that the used oil samples, both in diesel and H₂-assisted diesel engines, exhibit higher S2p BE values around 168 eV, confirming the presence of sulphates. This correlates with the observed depletion of the additive package (see Table 4), as sulphur-containing additives are known to oxidise under high-temperatures and high-pressures typical in engine operation conditions. The presence of sulphates in the tribofilm can influence its protective properties. Sulphates may alter the wear resistance and friction characteristics of the tribofilm and potentially lead to increased wear.

For the post-tribometric surfaces with used 5W30 low sulphated ash lubricant in a hydrogen-assisted diesel environment, the XPS results from wear track measurements show slightly higher atomic percentage of phosphate on average (5.53%), whilst 13.3% lesser zinc and 27.83% lesser sulphate content are noted (Figure 6). This observation can also provide an explanation for the lower measured coefficient of friction for the H₂-assisted diesel MTM tests under mixed regimes of lubrication. With reduced tribofilm formation the detection of 20.58% higher iron and 5.31% higher oxygen content (due to the formation of an oxide layer) can potentially be explained. It is noted that the atomic percentages of the detected phosphate, zinc and sulphide remain well below those formed by the fresh lubricant sample (i.e., 74.57%, 67.4%, and 82.5% lower respectively) (Figure 6).

The comparison of the results from the off-track and wear track shows that there is significantly higher atomic percentage of phosphate off-track in the case of H₂-assisted engine oil in comparison to the lubricant from the pure diesel-fuelled engines. In addition, a relatively small atomic percentage of zinc were observed off-

track for the H₂-assisted engine lubricant unlike the case for the diesel engine case, whilst there is also lower sulphate (9.24%) in the case of H₂-assisted engine oil tests. These are attributed to variabilities in the lubricants and tested conditions.

It is important to note that XPS is a surface-sensitive technique that probes only a few nanometres (typically 5–10 nm) into the depth of the surface. This shallow probing depth is advantageous for analysis of the outermost layers of the tribofilm, which are critical for understanding the chemical states and distribution of elements, contributing to lubrication and wear protection. It is noted that XPS alone cannot provide a complete understanding of the entire tribofilm thickness. It merely offers essential information about the surface chemistry. This data can be complemented with use of other techniques, such as Auger Electron Spectroscopy (AES) or Transmission Electron Microscopy (TEM), to obtain a more comprehensive understanding of the tribofilm's structure and thickness.

Concluding remarks

A comprehensive program of lubricant performance evaluation is reported, comprising in-field testing in 7.7 L diesel engines and the same engines converted to receive hydrogen assistance. The vehicles used were refuse trucks on regular scheduled duty rounds, traversing specified routes. Samples of used lubricants were collected in regular intervals of 2000 km from these vehicles, with the primary aim of ascertaining changes to the lubricant chemistry and rheology in the presence of hydrogen in the fuel mixture.

Unlike many reported laboratory or test-cell investigations, the study deals with realistic current dual-fuel engine configurations in normal operation. The study reports on the converted dual-fuel H₂-assisted diesel engines that are increasingly used in the UK by local authorities in their quest to meet their net zero emission targets. These engines may be regarded as “mildly” converted variants, using only up to 20% hydrogen mix at occasionally requested peak powers. Therefore, the study is practical and realistic albeit with some increased uncertainties, as opposed to many reported laboratory-based tests. The approach of using realistic “mild” H₂-assisted diesel engines currently in commercial fleets constitutes a novel contribution of the current study, as well as combined in-field- tribometric and analytical investigation.

The current study is specifically focused on an in-depth analysis of the performance of the lubricant in dual-fuel H₂-assisted engines, where there is currently a dearth of information. The collected lubricant samples were subjected to rigorous industry standard chemical evaluation and subsequently used for harsh controlled tribometric evaluation at high contact pressures and shear using an MTM.

The following specific conclusions can be drawn from the current analysis:

- The chemical analysis has shown only marginal changes in the lubricant's rheological state. This is potentially due to the relatively “mild” introduction/use of hydrogen in the investigated engines.
- The measured Stribeck data show only marginal differences in friction in fluid film regime of lubrication. This is attributed to the relatively low mileage of the used lubricants resulting in their relatively low shear degradation.
- Noticeable changes were observed in frictional behaviour of lubricant samples under mixed and boundary regimes of lubrication. In these cases, the lubricant from the H₂-assisted engine generated lower coefficient of friction compared with that of the diesel fuelled engine. In addition, both the used lubricants showed lower coefficients of friction than the fresh oil samples. These noted differences can potentially be attributed to the abilities of the lubricant samples in forming anti-wear tribo-films during tribometric tests as examined subsequently by XPS. However, a comprehensive conclusion can only be drawn with availability of further samples and test data.
- The differences in the anti-wear additives, adsorbed onto surfaces for diesel and H₂-assisted engine lubricant tests, showed only marginal differences, consistent with the observations from the lubricant chemical analysis. Therefore, the role of other factors, such as variations in surface topography and its evolution under the test conditions, as well as the need for more tests should be emphasised.

It is important to note that more lubricant samples at different stages of operation must be tested to achieve a more statistically significant set of results regarding the effect of hydrogen on lubricant performance, particularly in terms of constituent additives in the case of H₂-assisted diesel engines. The primary aim of this initial study is to highlight the need for a more thorough and in-depth study on the role of hydrogen fuel on the rheological and physiochemical properties of the lubricants and their interaction with the contiguous surfaces.

Acknowledgements

The authors would like to express their gratitude to the industrial collaborators of this research, mainly ULEMCO who provided hydrogen-assisted technology for the diesel ICEs, Castrol who provided lubricants for the field experiments, Aberdeen City Council for participation of their refuse trucks and SGS for providing chemical analysis of all lubricant samples. The support of Loughborough University Material Characterisation Centre (LMCC) through providing access to XPS is also acknowledged.


Declaration of conflicting interests


The authors declared no potential conflicts of interest with respect to the research, authorship, and/or publication of this article.

Funding

The authors received no financial support for the research, authorship, and/or publication of this article.

ORCID iDs

Ramin Rahmani  <https://orcid.org/0000-0002-6084-8842>

Robert Ian Taylor  <https://orcid.org/0000-0002-3132-8469>

References

- Chhugani T and Rahmani R. Full emissions and energy consumption life cycle assessment of different heavy-duty vehicles powered by electricity, hydrogen, methanol, and LNG fuels produced from various sources. *Energy Convers Manage* 2025; 326: 119439.
- Hydrogen Projects: planning barriers and solutions. Research Findings, UK Government, <https://assets.publishing.service.gov.uk/media/657a2a92095987000d95e086/hydrogen-projects-planning-barriers-and-solutions-report.pdf> (2023, latest access June 2024).
- Furuhama S and Fukuma T. High output power hydrogen engine with high pressure fuel injection, hot surface ignition and turbocharging. *Int J Hydrogen Energy* 1986; 11: 399–407.
- Verhelst S and Wallner T. Hydrogen-fueled internal combustion engines. *Prog Energy Combust Sci* 2009; 35: 490–527.
- Stepień Z. A comprehensive overview of hydrogen-fueled internal combustion engines: achievements and future challenges. *Energies* 2021; 14: 6504.
- Qin Z, Yang Z, Jia C, et al. Experimental study on combustion characteristics of diesel–hydrogen dual-fuel engine. *J Therm Anal Calorim* 2020; 142: 1483–1491.
- Mathai R, Malhotra RK, Subramanian KA, et al. Comparative evaluation of performance, emission, lubricant and deposit characteristics of spark ignition engine fueled with CNG and 18% hydrogen-CNG. *Int J Hydrogen Energy* 2012; 37: 6893–6900.
- Pardo-Garcia C, Orjuela-Abril S and Pabón-León J. Investigation of emission characteristics and lubrication oil properties in a dual diesel–hydrogen internal combustion engine. *Lubricants* 2022; 10: 59.
- Candelaresi D, Valente A, Iribarren D, et al. Comparative life cycle assessment of hydrogen-fuelled passenger cars. *Int J Hydrogen Energy* 2021; 46: 35961–35973.
- Rahmani R, Dolatabadi N and Rahnejat H. Multiphysics performance assessment of hydrogen fuelled engines. *Int J Engine Res* 2023; 24: 4169–4189.
- Project Coordinator Motor Vehicles and Road Transport. TUV Rheinland e.V. for the Federal Ministry for Research and Technology, Alternative energy sources for road transport – hydrogen drive test. Technical report, TUV Rheinland, 1990.
- McQueen JS, Gao H, Black ED, et al. Friction and wear of tribofilms formed by zinc dialkyl dithiophosphate antiwear additive in low viscosity engine oils. *Tribology Int* 2005; 38: 289–297.
- Umer J, Morris NJ, Rahmani R, et al. Effect of dispersant concentration with friction modifiers and anti-wear additives on the tribofilm composition and boundary friction. *J Tribology* 2021; 143: 111901.
- Leighton M, Morris N and Rahnejat H. Transient nanoscale tribofilm growth: analytical prediction and measurement. *Appl Sci* 2021; 11: 5890.
- Verhelst S and Sierens R. Hydrogen engine-specific properties. *Int J Hydrogen Energy* 2001; 26: 987–990.
- Umer J, Morris N, Leighton M, et al. Nano and microscale contact characteristics of tribofilms derived from fully formulated engine oil. *Tribology Int* 2019; 131: 620–630.
- Turturro A, Rahmani R, Rahnejat H, et al. Assessment of friction for cam-roller follower valve train system subjected to mixed non-Newtonian regime of lubrication. In: ASME internal combustion engine division spring technical conference, May 6, 2012, Vol. 44663, pp.917–923.
- Hertz H. Ueber die Berührung fester elastischer Körper. *J für die reine und angewandte Mathematik* 1882; 92: 156–171.
- Gohar R and Rahnejat H. *Fundamentals of tribology*. 3rd ed. London: World Scientific, 2018.
- Yu C, Meng X and Xie Y. Numerical simulation of the effects of coating on thermal elastohydrodynamic lubrication in cam/tappet contact. *Proc IMechE Part J: J Eng Tribol* 2017; 231: 221–239.
- Alakhramsing SS, de Rooij M, Schipper DJ, et al. Lubrication and frictional analysis of cam–roller follower mechanisms. *Proc IMechE Part J: J Eng Tribol* 2018; 232: 347–363.
- Chong WWF, Teodorescu M and Rahnejat H. Mixed thermo-elastohydrodynamic cam–tappet power loss in low-speed emission cycles. *Int J Engine Res* 2014; 15: 153–164.
- Hamrock BJ, Schmid SR and Jacobson BO. *Fundamentals of fluid film lubrication*. Boca Raton, USA: CRC Press, 2004.
- Greenwood JA. An extension of the Grubin theory of elastohydrodynamic lubrication. *J Phys, D: Appl Phys* 1972; 5: 2195.
- Alani K. The change in diesel engine oil properties during performance. *Technium* 2023; 13: 68–78.
- Dawczyk J, Morgan N, Russo J, et al. Film thickness and friction of ZDDP tribofilms. *Tribol Lett* 2019; 67: 34.
- Ueda M, Kadiric A and Spikes H. ZDDP Tribofilm formation on non-ferrous surfaces. *Tribol Online* 2020; 15: 318–331.
- Dörr N, Brenner J, Ristić A, et al. Correlation between engine oil degradation, tribochemistry, and tribological behavior with focus on ZDDP deterioration. *Tribol Lett* 2019; 67: 1–17.

Appendix

Nomenclature

Roman symbols

a	Hertzian contact radius (m)
E	Young's modulus of elasticity (Pa)
E^*	Composite modulus of elasticity (Pa)
E'	Equivalent modulus of elasticity (Pa)
G^*	Dimensionless materials' parameter (-)
G_e	Dimensionless elasticity parameter (-)
G_v	Dimensionless viscous parameter (-)
p	Contact pressure (Pa)
P_{max}	Maximum contact pressure (Pa)
R	Equivalent radius of curvature (m)
T	Temperature (°C)
U^*	Dimensionless speed parameter (-)
u	Speed of entraining motion (m/s)
W	Total applied normal load (N)
W^*	Dimensionless load parameter (-)

Greek symbols

α	Lubricant piezo-viscosity coefficient (Pa^{-1})
η_0	Dynamic viscosity at atmospheric pressure (Pa.s)
ν	Poisson's ratio (-)

Subscripts

b	Ball
d	Disc

Abbreviations

BE	Binding Energy
CNG	Compressed Natural Gas
CO	Carbon monoxide
CO ₂	Carbon dioxide
ECU	Electronic Control Unit
EHL	Elastohydrodynamic Lubrication

FMEP	Friction Mean Effective Pressure
ICE	Internal Combustion Engine
H ₂	Hydrogen
HC	Hydrocarbon
HDVs	Heavy Duty Vehicles
HICEs	Hydrogen fuelled Internal Combustion Engines
MTM	Mini-Traction Machine
PH	Potential (Power) of Hydrogen
SAPS	Sulphated Ash, Phosphorus, and Sulphur
SRR	Slide-roll ratio
TAN	Total Acid Number
TBN	Total Base Number
WLI	White Light Interferometry
XPS	X-ray Photoelectron Spectroscopy
ZDDP	Zinc dialkyldithiophosphate